Progress Report No. 6

INVESTIGATIONS OF ELECTRON EMISSION CHARACTERISTICS OF LOW WORK FUNCTION SURFACES

by

L. W. Swanson
A. E. Bell
L. C. Crouser

GPO PRICE $ _____

CFSTI PRICE(S) $ _____

Hard copy (HC) 2.00

Microfiche (MF) .50

ff 653 July 65

Prepared for

Headquarters
National Aeronautics and Space Administration
Washington, D.C

CONTRACT NASw-1082

FACILITY FORM 602

N66 27940 (ACCESSION NUMBER)	(THRU)
38 (PAGES)	1 (CODE)
CR-75630 (NASA CR OR TMX OR AD NUMBER)	26 (CATEGORY)

Field Emission Corporation

McMinnville, Oregon

NOTICE

This report was prepared as an account of Government sponsored work. Neither the United States, nor the National Aeronautics and Space Administration (NASA), nor any person acting on behalf of NASA:

A.) Makes any warranty or representation, expressed or implied, with respect to the accuracy, completeness, or usefulness of the information contained in this report, or that the use of any information, apparatus, method, or process disclosed in this report may not infringe privately owned rights; or

B.) Assumes any liabilities with respect to the use of, or for damages resulting from the use of any information, apparatus, method or process disclosed in this report.

As used above, "person acting on behalf of NASA" includes any employee or contractor of NASA, or employee of such contractor, to the extent that such employee or contractor of NASA, or employee of such contractor prepares, disseminates, or provides access to, any information pursuant to his employment or contract with such contractor.

Requests for copies of this report should be referred to

National Aeronautics and Space Administration
Office of Scientific and Technical Information
Attention: AFSS-A
Washington, D.C. 20546

INVESTIGATIONS OF ELECTRON EMISSION CHARACTERISTICS OF LOW WORK FUNCTION SURFACES

Report No. 6

by

L. W. Swanson
A. E. Bell
L. C. Crouser

Prepared for

Headquarters
National Aeronautics and Space Administration
Washington, D. C.

Quarterly Report No. 2
1 January to 31 March 1966

May 1966

CONTRACT NASw-1082

FIELD EMISSION CORPORATION
Melrose Avenue at Linke Street
McMinnville, Oregon 97128

TABLE OF CONTENTS

	Page
PURPOSE	1
ABSTRACT	2
ADSORPTION OF CESIUM FLUORIDE ON TUNGSTEN	3
Results and Discussion	5
SINGLE CRYSTAL FACE WORK FUNCTION AND ENERGY DISTRIBUTION MEASUREMENTS	11
Clean Tungsten Results	11
Zirconium-Oxygen Coated Tungsten	20
Conclusion	25
REFERENCES	31

LIST OF ILLUSTRATIONS

Figure 1. Curve (a) represents the variation of work function with heating temperature of a layer of cesium fluoride on tungsten. Sixty second heating times were used.

Curve (b) is the corresponding preexponential plot. B is defined by $B = \log \frac{a}{a_o}$ where a_o and a are the preexponential factors of the Fowler-Nordheim equation for clean and contaminated field emitters. 7

Figure 2. Variation in patterns of cesium fluoride adsorbed on tungsten and heated to various temperatures. 8

Figure 3. Curve (a) is a plot of work function versus cesium dose number for cesium adsorption on top of a layer of fluorine adsorbed on tungsten. 10

Figure 4. Field emission patterns of a (100) oriented tungsten emitter showing the alteration of the emission distribution before (photo a) and after (photo b) co-deposition of zirconium and oxygen. 12

Figure 5. Integral total energy distribution current from the <112> direction of a flash heated tungsten emitter plotted according to Equation 2. 14

Figure 6. Integral total energy distribution current from the <130> direction of a flash heated tungsten emitter plotted according to Equation 2. 15

Figure 7. Integral total energy distribution current from the <110> direction of an annealed ($T = 1000^{o}K$) tungsten emitter plotted according to Equation 2. The value of d = .280 eV.

Figure 8. (a) Curve shows the total energy distribution from the <100> direction of a tungsten emitter where d = 0.140 eV.

(b) Curve shows the total energy distribution from the <100> direction of a zirconium-oxygen coated tungsten emitter where d = 0.091 eV. 21

Figure 9. Integral total energy distribution current from the <100> direction of a zirconium-oxygen coated tungsten emitter plotted according to Equation 2. The value of d = 0.091 eV. 23

Figure 10. Curves show the total energy distribution from the <100> direction of a zirconium-oxygen coated tungsten emitter at the indicated values of p. The value of d = 0.091 eV. 24

Figure 11. Data points show the variation of the normalized half width of the total energy distribution with p for the <100> direction of a zirconium-oxygen coated tungsten emitter, where d = 0.091 eV. Solid line is the theoretical curve based on a free-electron model. 26

Figure 12. Data points show the variation of the position of the energy distribution peak height h on the energy axis ϵ_p with p for the <100> direction of a zirconium-oxygen coated tungsten emitter, where d = 0.091 eV. Solid line is the theoretical curve based on a free-electron model. 27

Figure 13. Data points show the variation of the total energy distribution peak height h with p for the <100> direction of a zirconium-oxygen coated tungsten emitter, where d = 0.091 eV. Solid line is the theoretical curve based on a free-electron model. 28

Figure 14. Curve (a) is the variation of the apparent work function of the (100) plane of a zirconium-oxygen coated tungsten emitter as determined by the Fowler-Nordheim slopes. Curve (b) gives the curve (a) results corrected for the T-F contribution to the field emission current. 29

PURPOSE

The primary aims of this investigation are to obtain an improved fundamental understanding of (1) the phenomena governing the production of low work function surfaces, and (2) the factors affecting the quality and stability of electron emission characteristics. It is expected that the information generated from this investigation will be relevant to various kinds of electron emission (i. e., photo, thermionic and field emission), although the primary emphasis will be placed upon field emission. Accordingly, field emission techniques will be employed, at least initially, to obtain the objectives of this work.

The formation of low work function surfaces will be accomplished by: (1) adsorption of appropriate electro-positive adsorbates, (2) co-adsorption of appropriate electro-positive and electro-negative adsorbates, and (3) fabrication of emitters of low work function surfaces from various metalloid compounds. Various properties of these surfaces to be investigated in order to obtain a more fundamental understanding of them are the temperature dependency of the emission and work function, the various types of energy exchanges accompanying emission, the energy distribution of the field emitted electron, and various aspects of the surface kinetics of adsorbed layers such as binding energy, surface mobility and effect of external fields.

ABSTRACT

27940

Co-adsorption studies of cesium and fluorine on tungsten have been initiated. Cesium adsorption and desorption occurs reversibly on top of a fluorine-tungsten layer. Pattern changes are nearly identical to cesium-oxygen co-adsorption on tungsten. Above 1000°K the cesium is removed from the fluorinated tungsten surface.

Careful energy distribution studies on the 112, 130, 110 and 100 planes of a clean and zirconium-oxygen coated tungsten emitter have been completed. Whereas the 130, 112 and 100 (when coated with zirconium) energy distribution results agree with the free electron theory of field emission, the 110 results yield anomalous values for the work function.

ADSORPTION OF CESIUM FLUORIDE ON TUNGSTEN

In the study of low work function adsorbates, the favorable properties of the alkali metals and alkaline earths have long been recognized. For cesium adsorbed on tungsten, work function decreases of approximately three volts have been obtained and even greater decreases were obtained when cesium was deposited on top of a chemisorbed layer of oxygen.[1, 2].

Field emission studies of the cesium/tungsten and cesium/oxygen/tungsten system are especially interesting since marked anisotropies in work function occur and these are readily detected in the field electron patterns. The anisotropies yield information about adsorbate coverages on different planes if assumptions about the dipole moments of the adsorbed complex on these regions can be made.

When cesium is adsorbed on a tungsten field emitter, the 110 planes preferentially adsorb cesium under equilibrium conditions to such an extent that these planes, although initially of very high work function, become the predominant electron emission areas until a coverage of 1.45×10^{14} atoms/cm^2 is reached at which point the (211) planes are equally bright. Deposition of cesium on top of a chemisorbed layer of oxygen, however, not only results in a lower minimum work function but alters electron emission anisotropy so that the 211 regions are the predominant electron emission regions when the cesium coverage is kept below that required to reach the work function minimum.

The presence of chemisorbed oxygen apparently lowers the work function of the cesium/tungsten adsorption complex by enhancing its dipole moment. Fluorine which is even more strongly electro-negative than oxygen is a likely candidate for effecting a similar decrease in ϕ_{MIN} and for this reason has been investigated here.

Gaseous fluorine is an awkward adsorbate to employ for the following reasons:

(1) It has a high chemical reactivity which results in handling problems.

(2) Its low boiling point precludes its use in condensation type sources.

(3) It is difficult to rid it of other low boiling point gases such as oxygen, nitrogen, carbon monoxide and hydrogen.

Consequently a search was made for a more convenient source of the gas. It was hoped that a chemical source could be obtained which would yield a flux of fluorine molecules when heated in vacuum Such sources have been successfully employed for the production in situ of oxygen and hydrogen. Cobalt trifluoride was finally considered for trial and a source receptacle consisting of a platinum bucket supported by nichrome heating leads was filled with the finely powdered compound and sealed into a standard field emission tube. After the tube had been processed by the usual evacuation and baking procedures, the platinum bucket was raised to a dull red heat and maintained at this temperature for several hours. The relatively high thermal capacity of the source bucket and its contents allowed the nichrome heating leads to be momentarily outgassed at bright red heat. In spite of these precautions taken to ensure outgassing of the source material, copious amounts of carbon monoxide were liberated when an attempt was made to dose the emitter with

fluorine. Continued heating of the source tended to deplete the supply but remaining uncertainties about the nature of the adsorbate - was it carbon monoxide, fluorine, a cobalt fluoride or a mixture of any or all of these - led to the abandonment of this approach to fluorine preparation.

Two other potential fluorine sources have been considered and one of them has now been successfully used. In both of these methods a binary fluorine compound is deposited on the emitter and the fluorine is left behind when the emitter is heated. The compound used in this work is cesium fluoride which is sufficiently volatile to be deposited by heating a platinum bucket containing it to a dull red heat. The amount of fluorine deposited in a single dosing sequence is probably determined by the size of the cesium atoms of which about one cesium atom to every four tungsten atoms is enough to constitute a monolayer of adsorbate. A greater concentration of fluorine than one fluorine atom to every four surface tungsten atoms can be achieved by removing the cesium from the first dose and redepositing more cesium fluoride and then heating the adsorbate layer to $\sim 1000^{o}K$. Because of the need to heat to this temperature it is likely that the resultant fluorine layer will be incomplete; it is also possible that substrate changes are induced by such heat treatment. A source of fluorine that would possibly circumvent this problem is xenon hexafluoride which has a vapor pressure of 30 mm at $25^{o}C$. The hexafluoride would decompose on the emitter and liberate the xenon probably below room temperature.

Results and Discussion. A layer of cesium fluoride was deposited on the emitter by dosing while viewing the field emission pattern intermittently. Equilibration of the dose was established by heating to $420^{o}K$ for 60 seconds.

At this point, a minimum work function of 1.52 eV was obtained (see Figure 1.) Heating at gradually increasing temperatures up to 1000°K resulted in an increase in work function from 1.52 to 4.75 eV, and beyond this point resulted in a decline from 4.75 to 4.52 eV at 1770°K. Heating times of 60 seconds were used except for the last few steps, in which case heating times of 30 seconds were used. No bias voltage was applied to the screen so that both ionic and neutral desorption occurred simultaneously. The corresponding pre-exponential changes are also included in Figure 1. This shows that the pre-exponential increased when the cesium fluoride was deposited, declined to a value less than that of clean tungsten at 950°K and then after an increase of 970°K remained constant until 1600°K, beyond which it reverted to the clean tungsten value.

Wolf[3] has obtained a similar work function desorption curve in a field emission study of cesium fluoride desorption from tungsten. He, however, obtained a lower minimum (1.1 eV) and a greater maximum work function (5.1 eV) than described above. The less extreme values described here are probably a consequence of an initial dose that was less than a monolayer. Field electron pattern changes (see Figure 2) for cesium fluoride on tungsten were very similar to those obtained for cesium adsorption on oxygenated tungsten; in both cases the 211 regions were the most strongly emitting areas. In other respects the desorption curves were very similar. The increase in work function from 550°K to 970°K and the corresponding decrease in pre-exponential, are interpreted to be due to evaporation of cesium first in the form of atoms and then finally as ions. Beyond 1000°K it is thought that only fluorine remains on the emitter until a temperature of 1600°K is reached at which point fluorine begins to desorb. The final

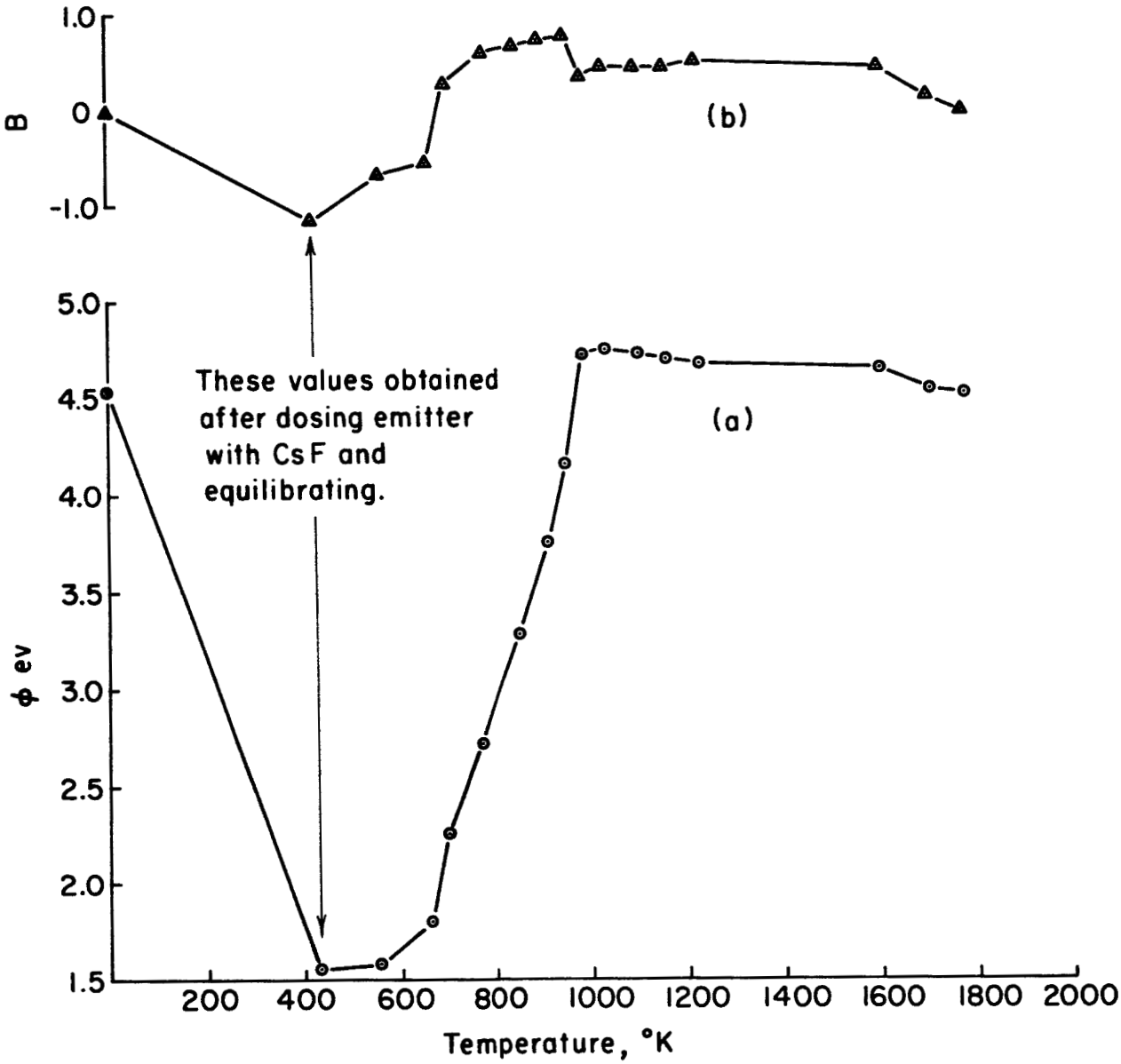

Figure 1. Curve (a) represents the variation of work function with heating temperature of a layer of cesium fluoride on tungsten. Sixty second heating times were used.

Curve (b) is the corresponding preexponential plot. B is defined by $B = \log \frac{a}{a_o}$ where a_o and a are the preexponential factors of the Fowler Nordheim equation for clean and contaminated field emitters.

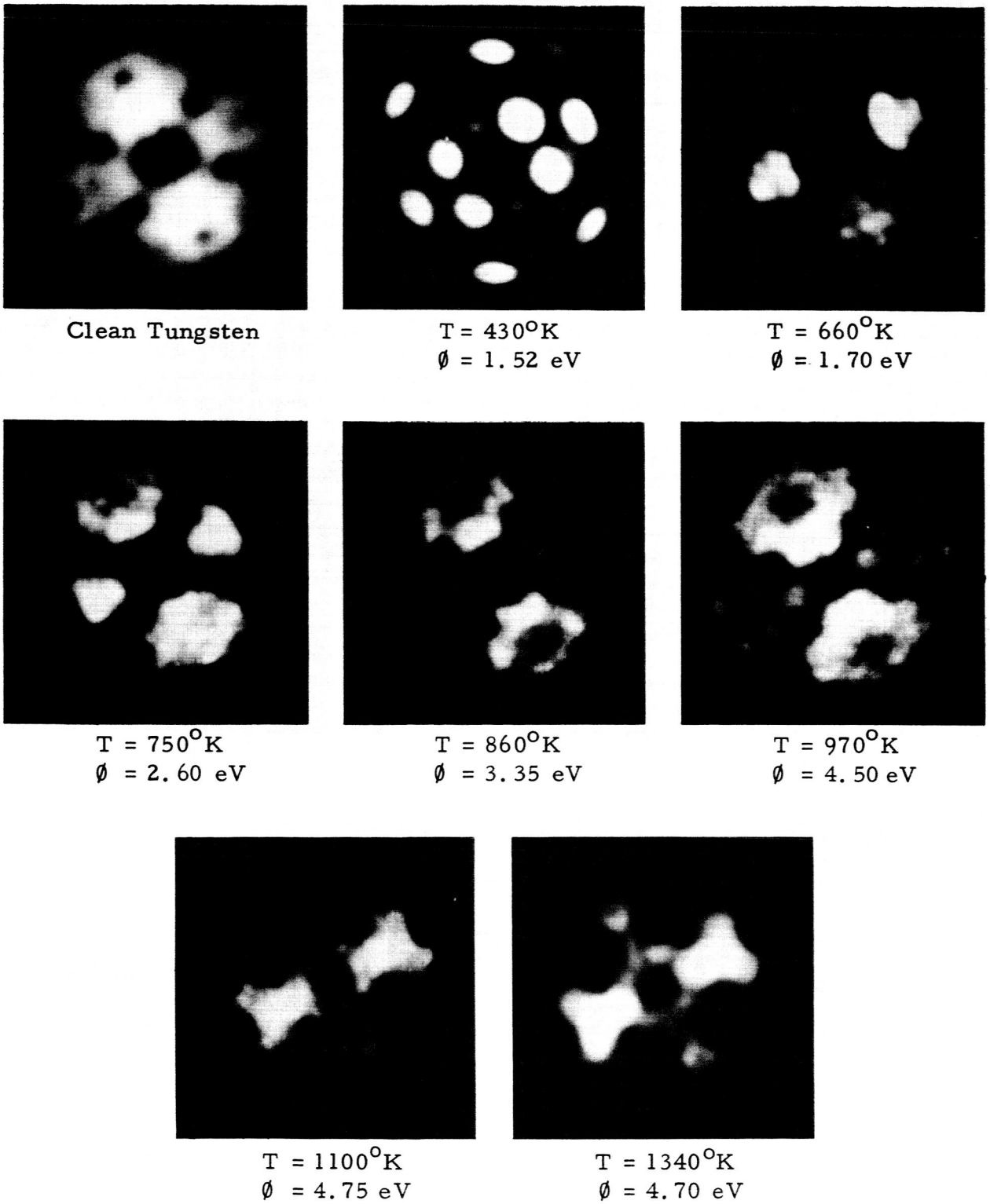

Figure 2. Variation in patterns of cesium fluoride adsorbed on tungsten and heated to various temperatures.

desorption temperature of cesium (950-990°K) was somewhat greater than that required to remove cesium from a clean tungsten surface (900-930°K) but corresponds to that required to remove cesium from an oxygenated tungsten surface of initial work function 4.55 eV.

By repeating the procedure of depositing fluorine five times it was hoped that a much greater coverage of fluorine could be obtained. However, the resulting work function of 4.8 eV was significantly lower than that obtained by Wolf who obtained a value of 5.1 eV by maintaining an emitter at 1200°K while dosing. Apparently the latter procedure is considerably more effective in establishing a high fluorine coverage.

Results of dosing with cesium the emitter treated in this way are shown in Figure 3. Throughout the coverage range, a temperature of 220°K was found sufficient to effect apparent equilibration as judged by field emission patterns. Since this temperature is considerably below that required for equilibration of cesium on tungsten or oxygenated tungsten it seems likely that true equilibrium was not attained. This situation has been reported before[4] and is due to the fact that true equilibration which necessitates establishment of equilibrium between shank and emitter involves diffusion of adsorbate over distances of the order of 1 mm whereas local equilibration of adsorbate on the emitter involves diffusion over distances of the order of only 1000 Å.

The absence of a minimum in the curve of work function coverage curve of Figure 3 is probably due to insufficient dosage of cesium to attain a monolayer coverage. Further investigations of this nature will be performed.

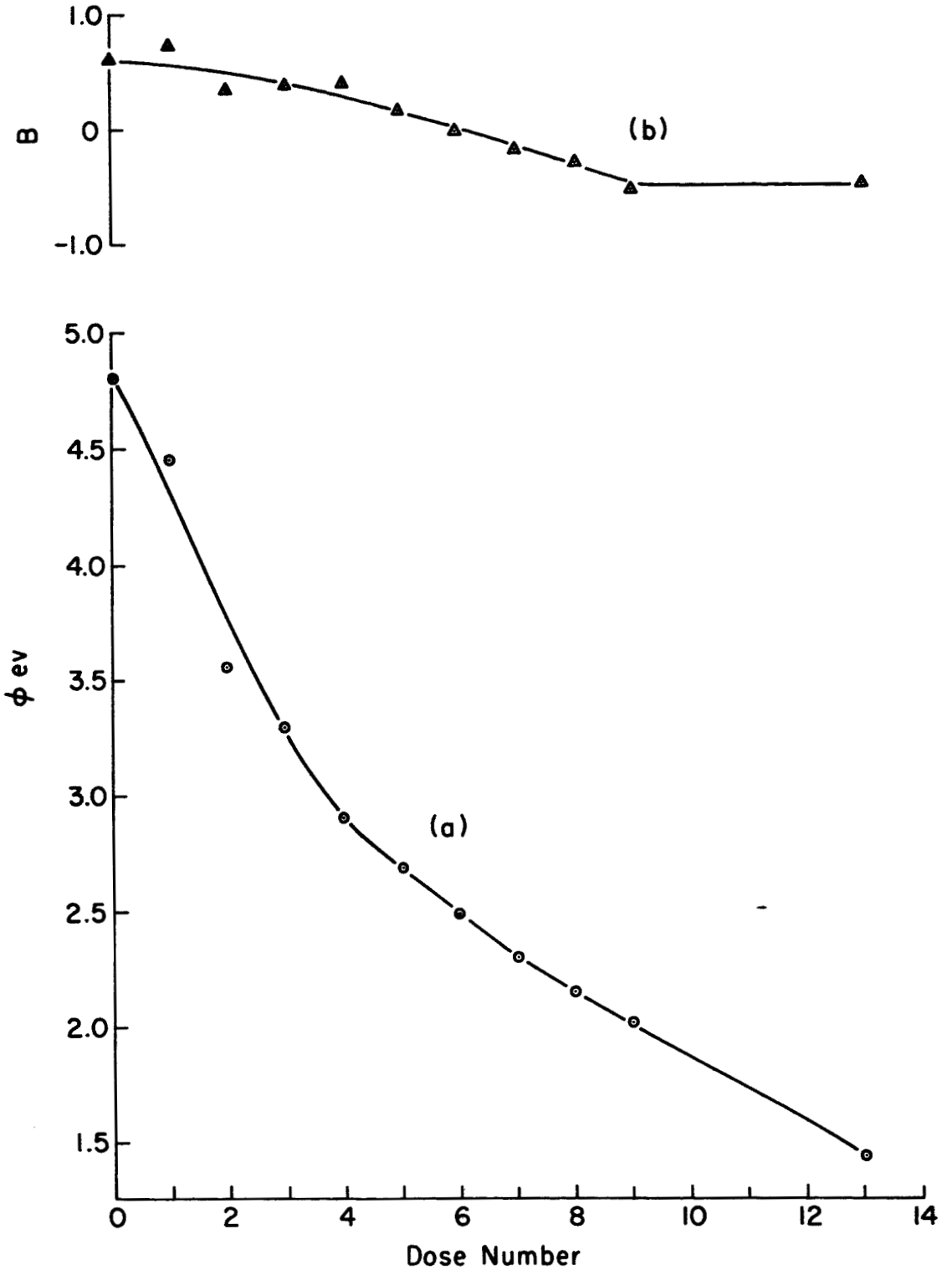

Figure 3. Curve (a) is a plot of work function versus cesium dose number for cesium adsorption on top of a layer of fluorine adsorbed on tungsten.

Curve (b) is the corresponding preexponential plot.

SINGLE CRYSTAL FACE WORK FUNCTION AND ENERGY DISTRIBUTION MEASUREMENTS

During the past quarter further measurements of the energy distribution and work function for field emitted electrons from various planes of clean- and zirconium-coated tungsten have been completed. The main purpose for this continued work was to analyze the energy distribution and Fowler-Nordheim data by a method described previously[5] which yields an independent value for work function ϕ and field factor $\beta = F/V$ where F and V are the applied field and voltage respectively. In addition, an investigation of the influence of a low work function coating, consisting of coadsorbed oxygen and zirconium, on the energy distribution characteristics has been completed. Figure 4 shows a typical field electron pattern of a zirconium-oxygen coated tungsten emitter and illustrates the very specific lowering of the (100) work function.

There are several interesting questions regarding the behavior of the zirconium-oxygen layer on tungsten. First the effect of this adsorbed layer on the anomaly noted in the clean (100) energy distribution results may shed light on its cause; second, there has been some uncertainty as to the absolute value of the work function due to possible local geometric arrangement which may be clarified by the energy distribution studies; and third, the temperature dependence of the work function of a zirconium-oxygen coated tungsten surface will be of intrinsic interest to the overall understanding of the system.

Clean Tungsten Results. From earlier discussions[5] it was shown that from the slope m_f of the Fowler-Nordheim plot and the slope m_e of the plot of the

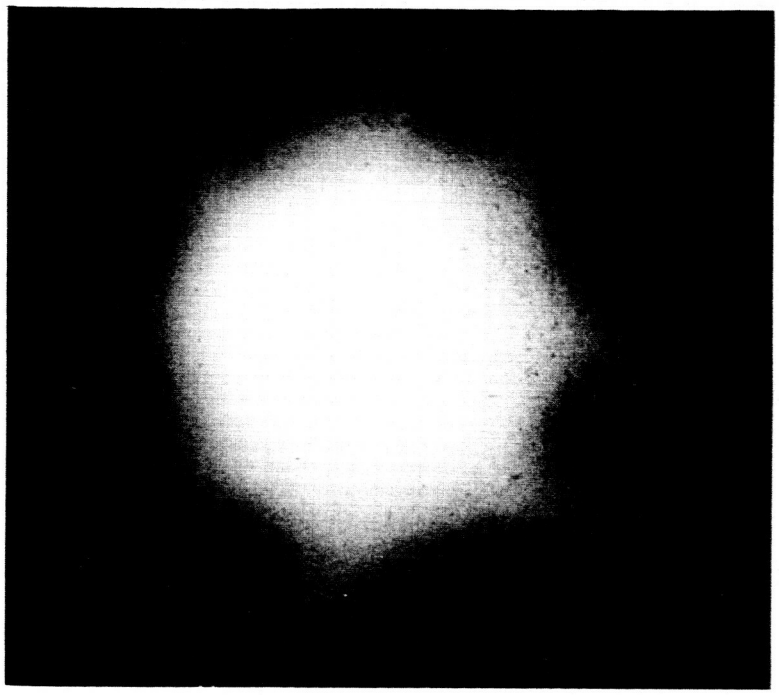

(a)

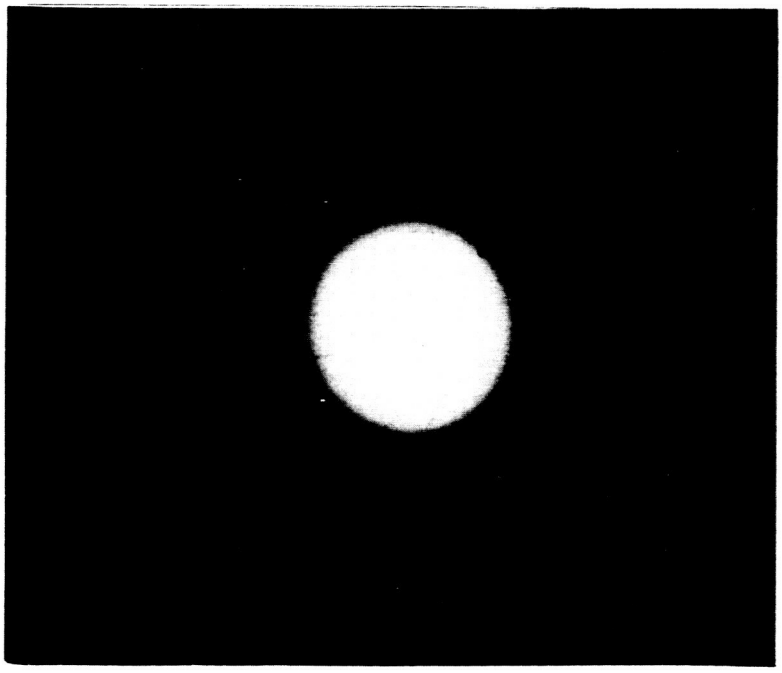

(b)

Figure 4. Field emission patterns of a (100) oriented tungsten emitter showing the alteration of the emission distribution before (photo a) and after (photo b) co-deposition of zirconium and oxygen.

integral energy distribution current in the form $\ln(I-I_o)$ vs V_t(where I_o is the saturated collector current and V_t is the emitter to collector bias voltage), one can obtain an expression for the work function ϕ_e as follows:

$$\phi_e = \frac{3\ m_f\ t(y)}{2\ m_e V\ s(y)} \tag{1}$$

where t(y) and s(y) are tabulated functions[6] and V the emitter to anode voltage.

Plots of the integral curves for the <112><130> and <110> directions are given in Figures 5 - 7 according to the equation:

$$\ln\frac{I-I_o}{I_o} = -\frac{\epsilon}{d} \tag{2}$$

where $\epsilon = -V_t - E_f$. Equation (2) is valid in the range $\exp(\epsilon/pd) < 1$, where $p = kT/d$ and $d = heF/2(2m\phi)^{1/2}t(y)$. From the Figure 5 - 7 results it is evident that Equation (2) is obeyed and that the free electron behavior is upheld along these directions. However, the stringent test is in the evaluation of the work function according to Equation (1). From Table I the values of ϕ for the (112) and (130) are in close agreement with the work functions evaluated according to plots of the I(V) data according to the Fowler-Nordheim equation, namely

$$m_f = 2.83 \times 10^7 \phi^{3/2}/\beta \tag{3}$$

or

$$\phi_f = \overline{\phi}_f \left(\frac{m_f\ \beta}{\overline{m_f}\ \overline{\beta}}\right)^{2/3} \tag{4}$$

where m_f and $\overline{m_f}$ are the slopes of the respective Fowler-Nordheim plots of the probe and total currents and where $\overline{\phi_f} = 4.52$ eV. In contrast, the value

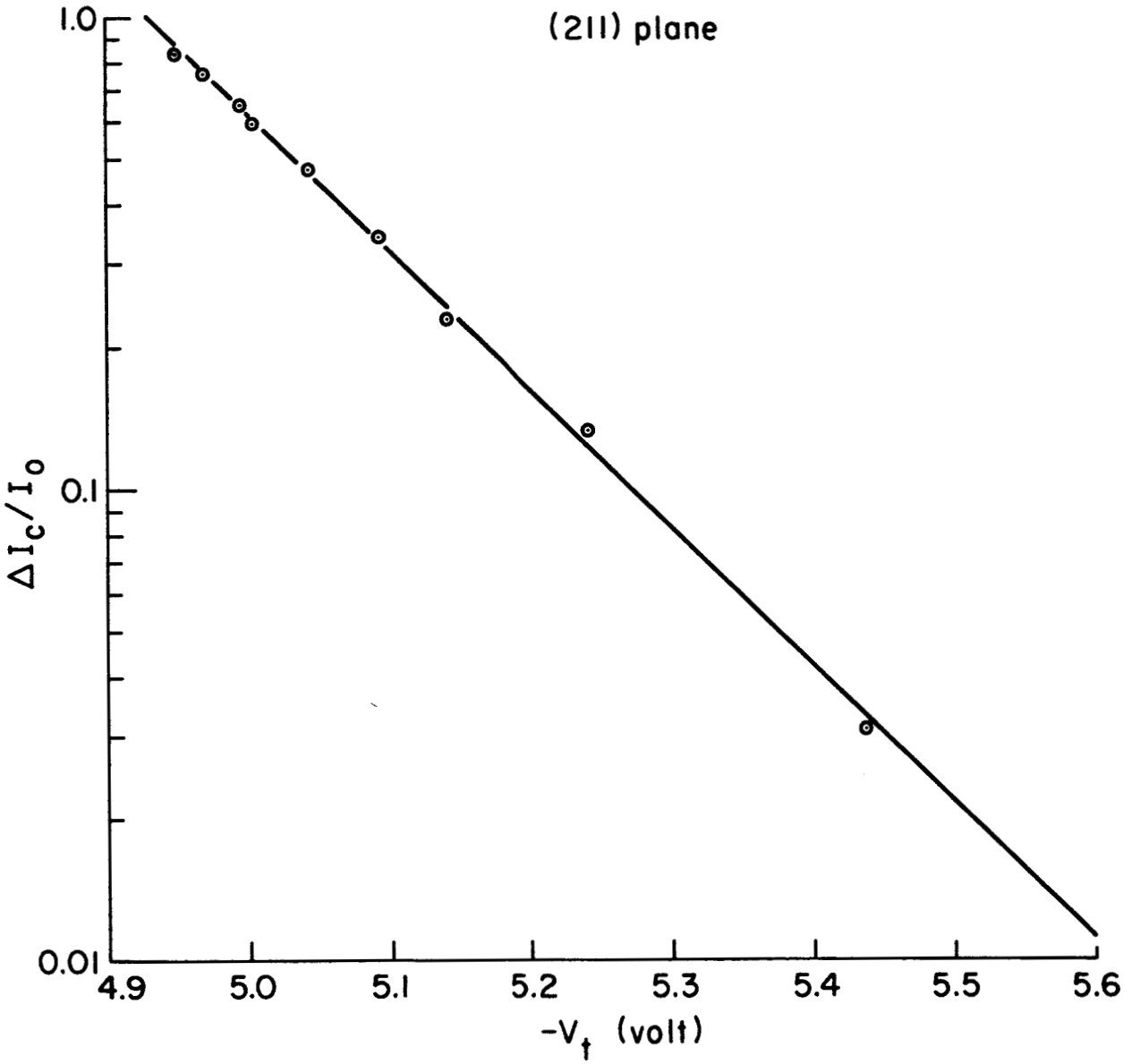

Figure 5. Integral total energy distribution current from the ⟨112⟩ direction of a flash heated tungsten emitter plotted according to Equation 2.

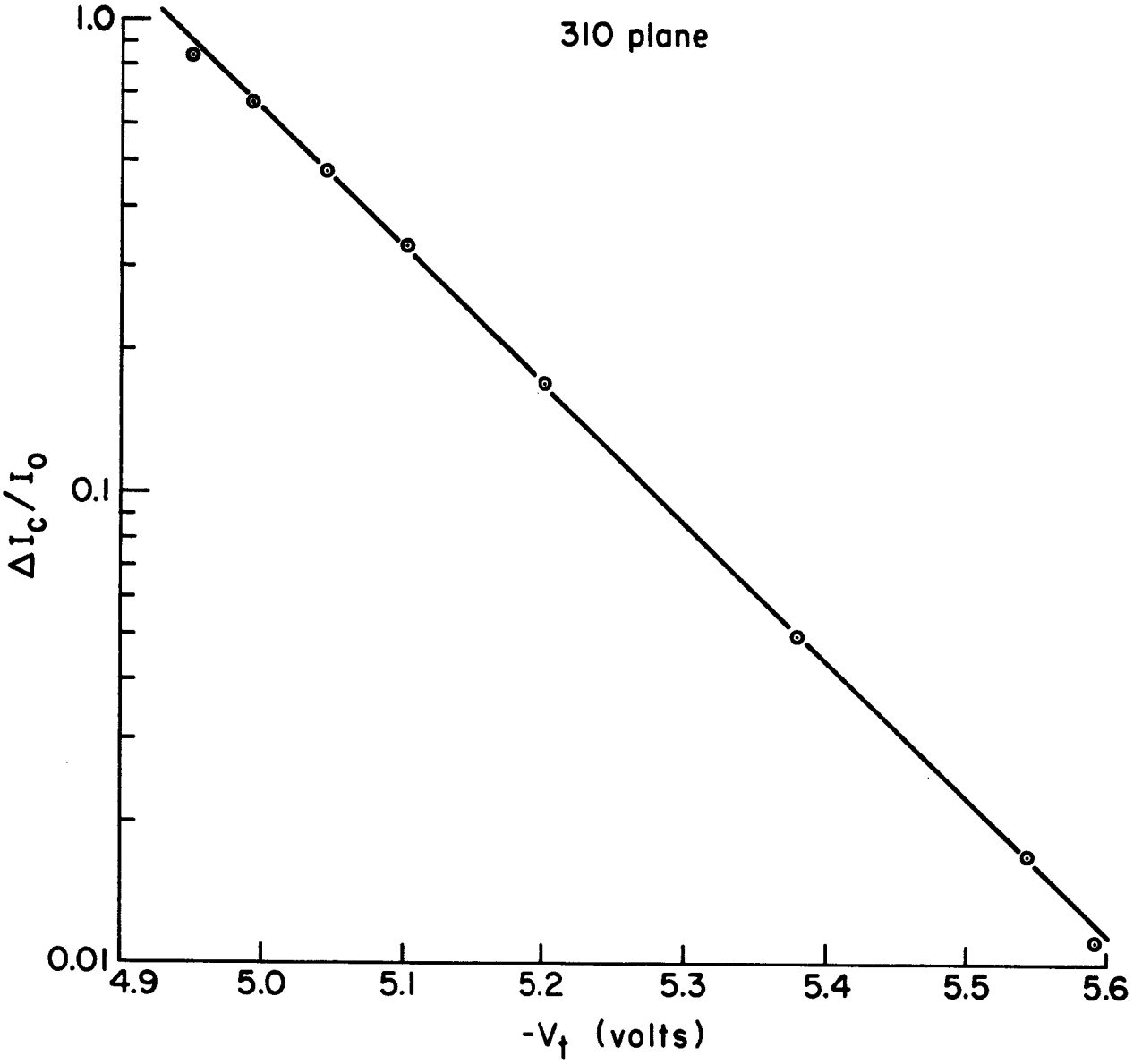

Figure 6. Integral total energy distribution current from the ⟨130⟩ direction of a flash heated tungsten emitter plotted according to Equation 2.

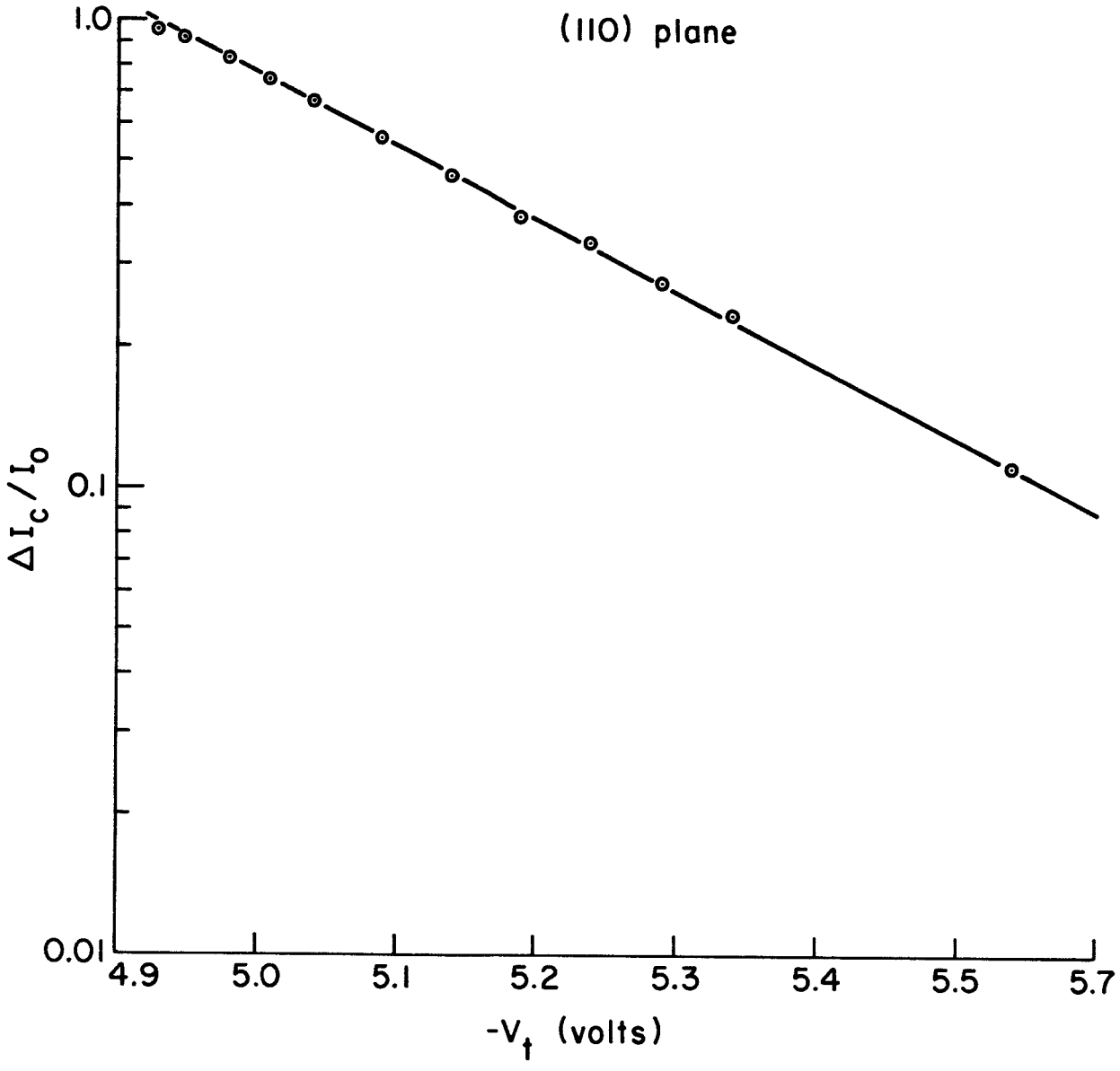

Figure 7. Integral total energy distribution current from the ⟨110⟩ direction of an annealed (T = 1000°K) tungsten emitter plotted according to Equation 2. The value of d = 0.280 eV.

TABLE I

Clean Tungsten Results

Plane	ϕ_e(eV)	ϕ_f(eV)*	$\overline{\phi_f}$(eV)	$\beta / \overline{\beta}$	M($\times 10^5$)
112 (flashed)	5.14	4.94	4.52	1.09	1.01
112 (annealed)	5.16	4.92	4.52	1.07	1.43
130 (flashed)	4.37	4.20	4.52	1.07	2.66
130 (annealed)	4.38	4.30	4.52	1.03	2.66
100 (annealed)	--	4.68	4.52	--	3.30
110 (annealed)	7.85	5.00	4.52	1.95	17.1
111 (annealed)	--	4.42	4.52	--	1.74

Zirconium-Coated Tungsten Results

130 (annealed)	4.03	3.76	3.00	1.11	15.6
100 (annealed)	2.25	2.70	2.81	0.72	10.5

*Work functions are corrected for variations in β with angular separation from apex (see reference 5).

of ϕ_e for the <110> direction is considerably higher than the ϕ_f value. It is moreover interesting that the value $\phi_f = 5.0$ for the <110> direction, rather than the customary 5.8 to 6.0 eV value obtained from <110> oriented emitters. We have observed these values of ϕ_f for both <130> and <100> oriented emitters whereas for <110> oriented emitters the value obtained for ϕ_f is always in the 5.8 to 6.0 eV range. It is not clear at this time why the emitter orientation should make such a profound difference in the value of ϕ_f for the 110 plane; since ϕ_f values of other planes are unaffected by emitter orientation, it is clear that the high value of ϕ_f of the 110 plane cannot be attributed to an orientational effect on the $\overline{\phi_f}$. The remaining possibility is a variation in local field factor β since in this case Equation (4) becomes

$$\phi_f = \overline{\phi_f} \left(\frac{m_f \beta}{\overline{m_f \beta}} \right)^{2/3} \tag{5}$$

Thus if $\beta < \overline{\beta}$ for a 110 plane when the orientation is <110> the higher value of ϕ_f obtained for this orientation would be reduced by $(\beta/\overline{\beta})^{2/3}$. It is well known that the (110) plane possesses a rather large size thereby causing a degree of flattening or faceting along this direction of the hemispherical emitter. Müller[7] has estimated that a 110 plane subtending an angle of 7 - 10° can be accountable for a 6 - 14% reduction in β. There is no obvious reason at the moment to believe this faceting for a given plane to be greatly dependent on the emitter orientation. On the basis of the variation of surface free energy with radius of curvature one might expect a larger 110 facet when it is not at the emitter apex. This of course is in opposition with the direction of the effect necessary to explain the observed results. The (110) plane of a non-

<110> oriented emitter must exhibit a value of $\beta/\overline{\beta} \sim 10\%$ below that of an on-axis (110) plane in order to account for the observed experimental variations in work function. It is interesting that all thermionic, surface ionization and retarding potential measurements of the (110) plane work function range in value from the 5.0 to 5.3 eV, which is close to the value we obtained for the non-110 oriented emitter by the Fowler-Nordheim slope method.

A most striking result shown in Table I is the anomalously high value of the 110 work function obtained from analysis of the Figure 7 results according to Equation (1). We have recently learned that Dr. Young of the Bureau of Standards obtained a similarly high value (8.7 eV) by this method for a <110> oriented emitter. If this anomalous value arises from band structure effects, as suggested earlier[8,9] for the 100 results, it is peculiar that this effect only alters the slope of the Figure 7 plot (and not the shape), whereas for the 100 results the shape is significantly altered. Additional evidence that the energy distribution results for the 110 are not in accord with theory is given by the unusually large value of $\beta/\overline{\beta}$. Further theoretical investigation will be necessary to understand the meaning of these results in terms of the expected Fermi surface shape. According to existing ideas of the Fermi surface topology a small hole surface intersects Brillouin zone along the <110> direction and may be the cause of the anomalous value of ϕ_e for the (110) plane.

The values of ϕ_f and β obtained for the 112 and 130 planes are slightly larger than average. Little effect is noted in ϕ_f as obtained via Equation(3) upon annealing the surface (although a slight decrease in $\beta/\overline{\beta}$ is observed on the annealed surface for the 130 plane). It is therefore believed that a large

amount of apparent variation in the Fowler-Nordheim evaluated work functions with annealing temperature is caused by thermodynamically motivated variations in net plane size.

The last column in Table I gives the linear magnification as determined by

$$M = \left(\frac{A_p}{A_f}\right)^{1/2} \tag{6}$$

where A_p and A_f are areas of the probe hole and the emitting surface (as determined from analysis of the intercept of the Fowler-Nordheim plots) respectively. No particular relationship between M and $\beta/\overline{\beta}$ is observed with these data. The large increase in M on the (110) plane is difficult to understand and cannot be explained at this time. For <110> oriented emitters we do not observe such an increase in M on the 110 plane.

Zirconium-Oxygen Coated Tungsten. Investigation of the emission characteristics of a zirconium-oxygen coated emitter were performed by coating a <130> oriented emitter with zirconium and oxygen from a suitable source. The striking alteration of the emission distribution, as shown in Figure 4, has been reported and discussed in other reports.[10] The half width, $d_{1/2}$ of the energy distribution at $T = 0^{o}K$ is given by

$$d_{1/2} = 0.69d \tag{7}$$

At a constant current density $\phi^{3/2}/F$ = const which when combined with Equation (7) yields

$$d_{1/2} = \text{const}\ \phi \tag{8}$$

Thus we can expect a reduction in $d_{1/2}$ as ϕ is decreased. Figure 8 shows

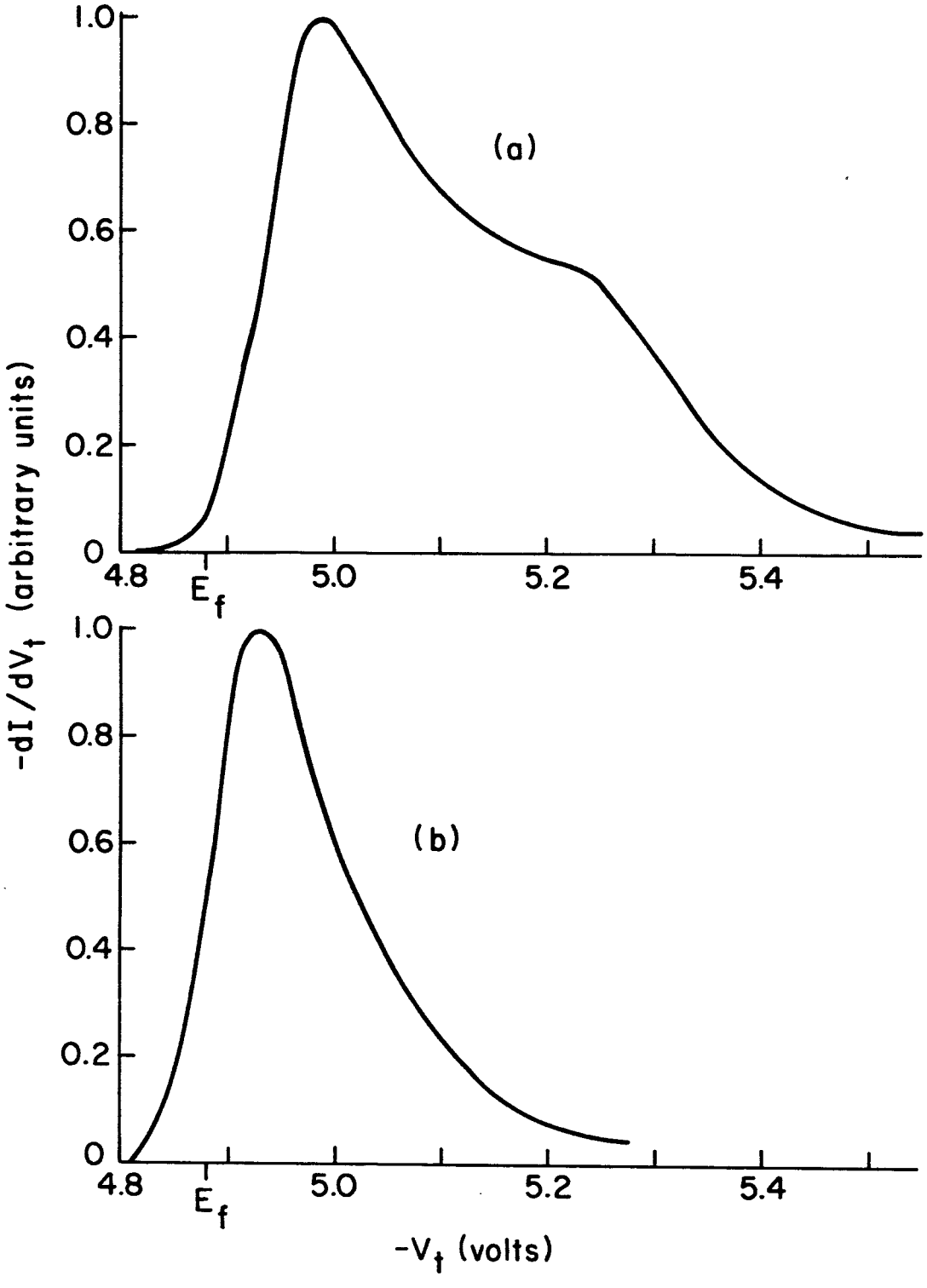

Figure 8(a) Curve shows the total energy distribution from the ⟨100⟩ direction of a tungsten emitter where d = 0.140 eV.

Figure 8(b) Curve shows the total energy distribution from the ⟨100⟩ direction of a zirconium-oxygen coated tungsten emitter where d = 0.091 eV.

the experimental energy distribution obtained on a clean zirconium-oxygen coated tungsten emitter. It is clear that a reduction in $d_{1/2}$ has taken place; moreover the zirconium-oxygen coated energy distribution does not exhibit the anomalous shoulder shown in the clean tungsten results. Because the shoulder occurs at 0.35 eV below the Fermi level and in the case of the zirconium coating at this value of V_t the distribution has already fallen to a very low value, it was concluded that the energy range where the anomaly occurs is not reached with the low work function surface. Table I shows the values of ϕ_e and $\beta/\overline{\beta}$ obtained on the (100) and (130) planes via Equation (1). Figure 9 shows the plot of the 100 data for the zirconium coated emitter according to Equation (2). The large increase in $\beta/\overline{\beta}$ on the (130) and (100) planes respectively and the large increase in M upon adsorption of zirconium is indicative of a significant rearrangement of the substrate geometry. The localization of the work function change to the (100) plane upon adsorption is apparent by noting that the 100 work function is decreased by 2.4 eV whereas the 130 work function is diminished by only 0.34 eV. It is interesting that both the 100 and 130 planes exhibit a large increase in M on zirconium adsorption.

Because of the anomalous energy distribution on the (100) plane, one may question the validity of the 2.25 eV work function obtained in Equation (1), even though the fit of the data to Equation (1) is quite adequate. In an attempt to ascertain the correct value of the work function, the variation of the energy distribution with the temperature was measured and plotted in Figure 10. The values of ϕ obtained both by Equation (1) and Equation (4) (assuming $\beta/\overline{\beta} = 1$) were used to calculate p. Inasmuch as the value of p = 1/2 according to theory leads to a symmetrical energy distribution, it was possible to determine

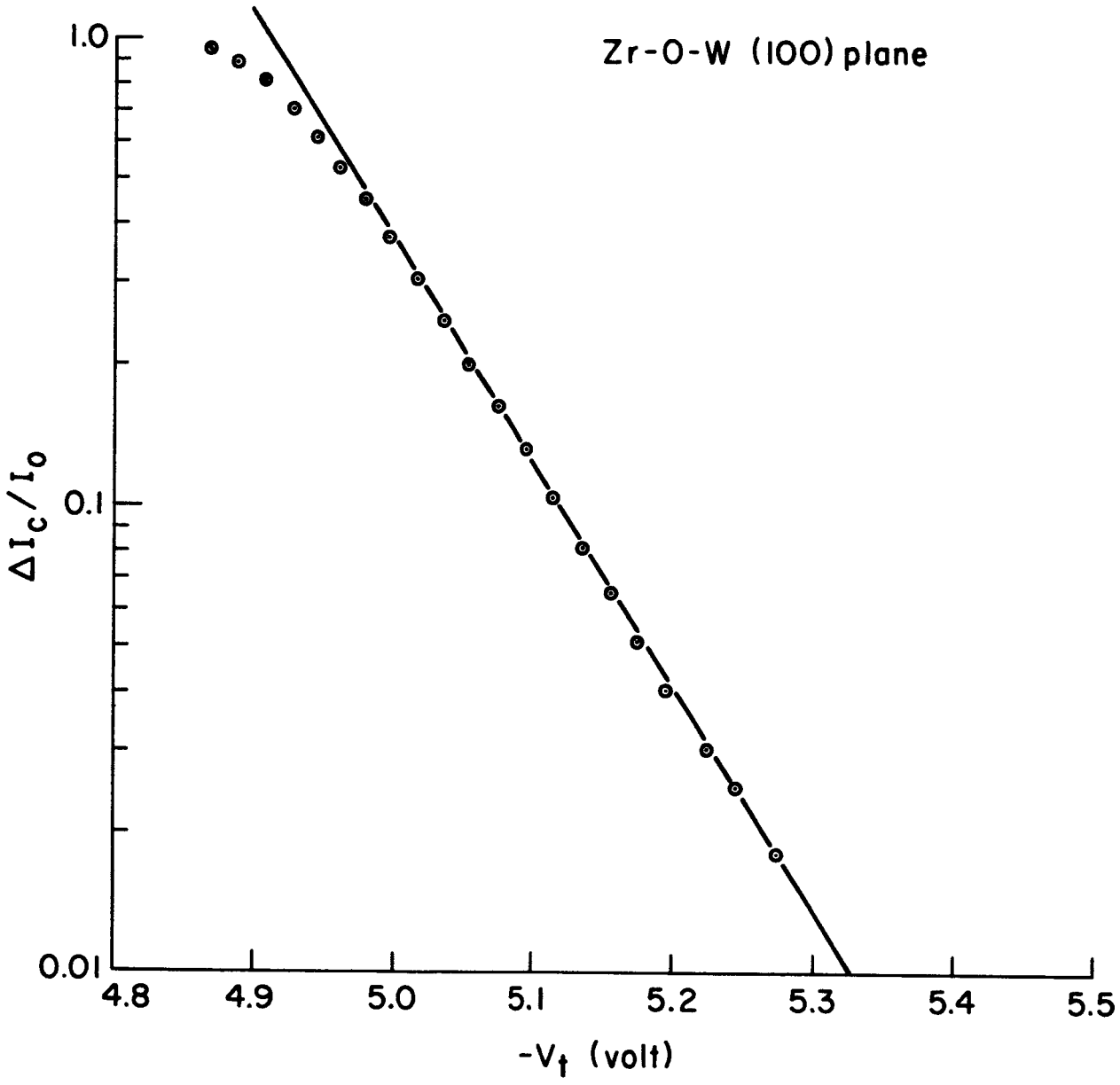

Figure 9. Integral total energy distribution current from the ⟨100⟩ direction of a zirconium-oxygen coated tungsten emitter plotted according to Equation 2. The value of d = 0.091 eV.

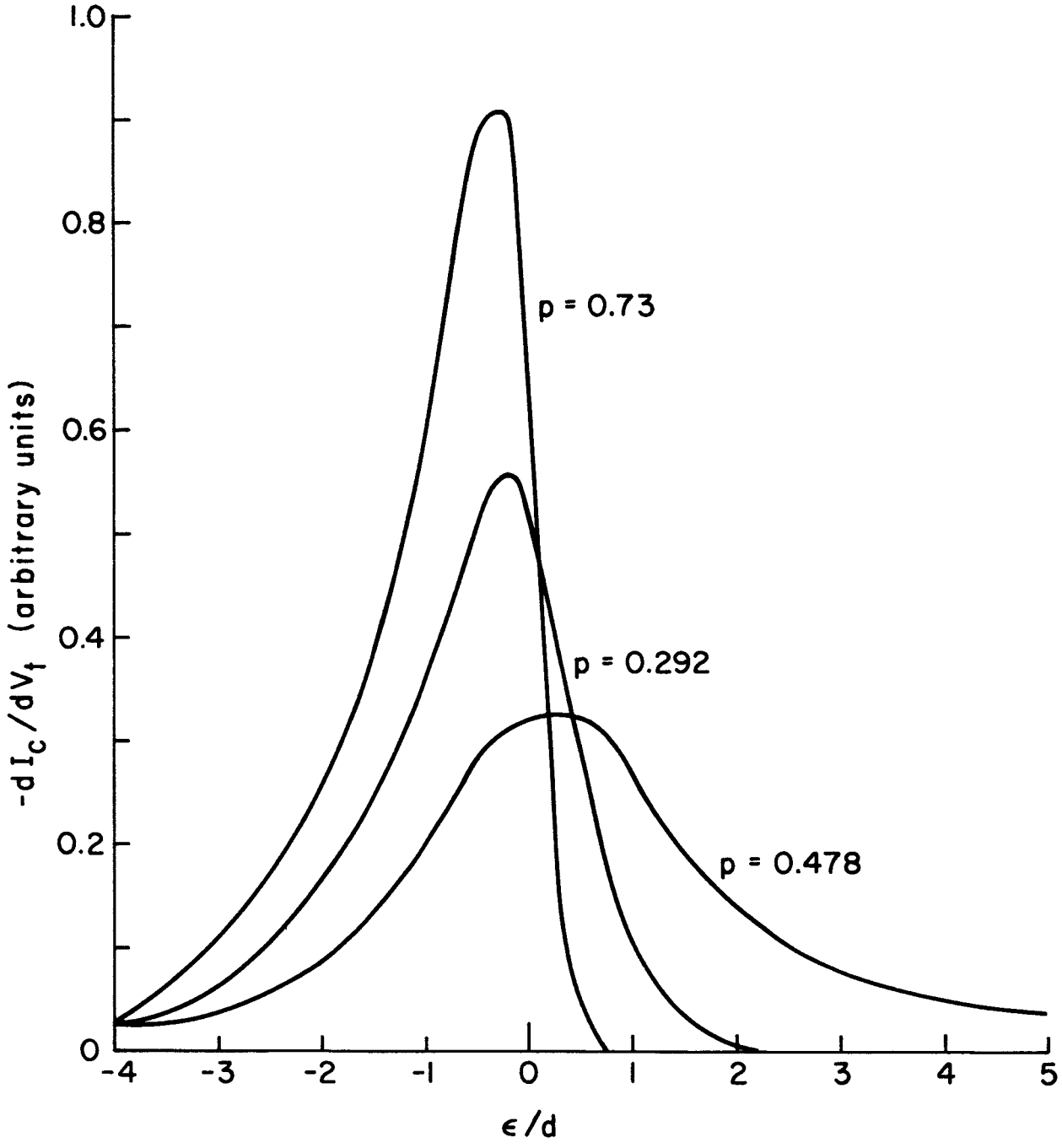

Figure 10. Curves show the total energy distribution from the<100>direction of a zirconium-oxygen coated tungsten emitter at the indicated values of p. The value of d = 0.091 eV.

the correct value of p and hence ϕ. Accordingly, as shown in Figure 10, the lower value of ϕ_e = 2.25 eV and $\beta/\bar{\beta}$ = 0.72 provide the correct value of p = 0.48 at the near symmetrical distribution whereas the Fowler-Nordheim work function ϕ_f = 2.70 eV with $\beta/\bar{\beta}$ = 1 yields p = 0.38. In order to further compare the energy distribution results with theory, Figures 11 through 13 show plots of the energy distribution half width $d_{1/2}$, the position of the energy distribution peak ϵ_p on the energy axis and the peak height h all as a function of p. The overall self consistency and the fit of the data to theory for the respective curves is sufficiently close to conclude that the energy distribution theory (neglecting band structure effects) is upheld on the (100) plane when a low work function adsorbate is present.

Plotted in Figure 14 is the variation of the work function with temperature for the (100) plane of a zirconium-oxygen coated emitter. From previous work[9] it was shown that the clean (100) plane work function exhibited a negative temperature coefficient of $d\phi/dT = -10.9 \times 10^{-5}$ eV/°K. Figure 14 shows both the work function variation obtained from the variation of the Fowler-Nordheim slope with temperature using the 0°K approximation and the latter corrected for the T-F contribution to the field emission. Upon making the latter correction it is observed that the temperature coefficient of the coated 100 surface is zero within experimental error.

Conclusion. The (112) and (130) planes yielded energy distributions from which a sensible work function could be extracted. The energy distribution from the (110) plane, on the other hand, fits the theory but yields an anomalously high value of work function. Coadsorbed zirconium and oxygen on tungsten restores the proper shape to the energy distribution from the <100> direction.

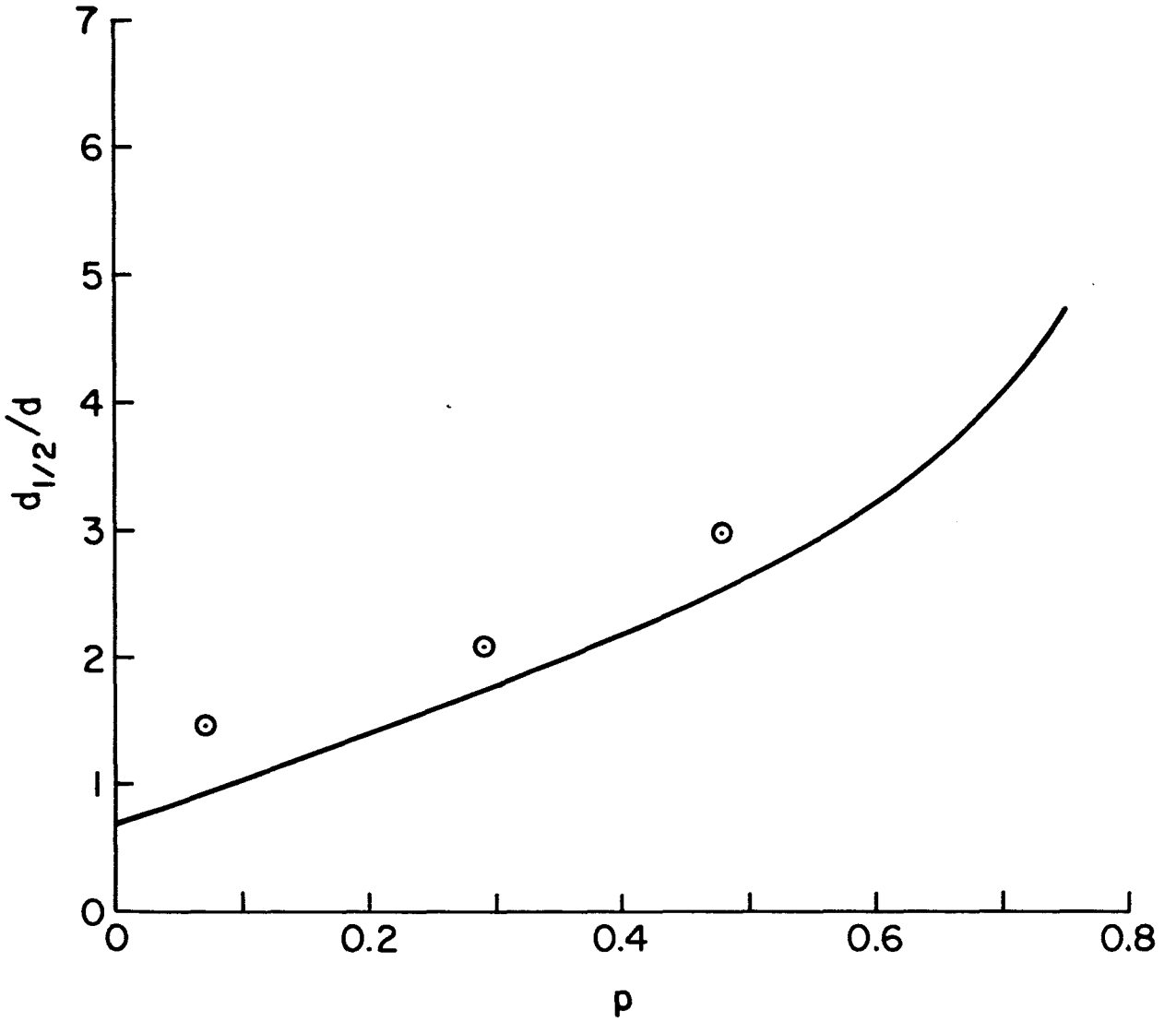

Figure 11. Data points show the variation of the normalized half width of the total energy distribution with p for the ⟨100⟩ direction of a zirconium-oxygen coated tungsten emitter, where d = 0.091 eV. Solid line is the theoretical curve based on a free-electron model.

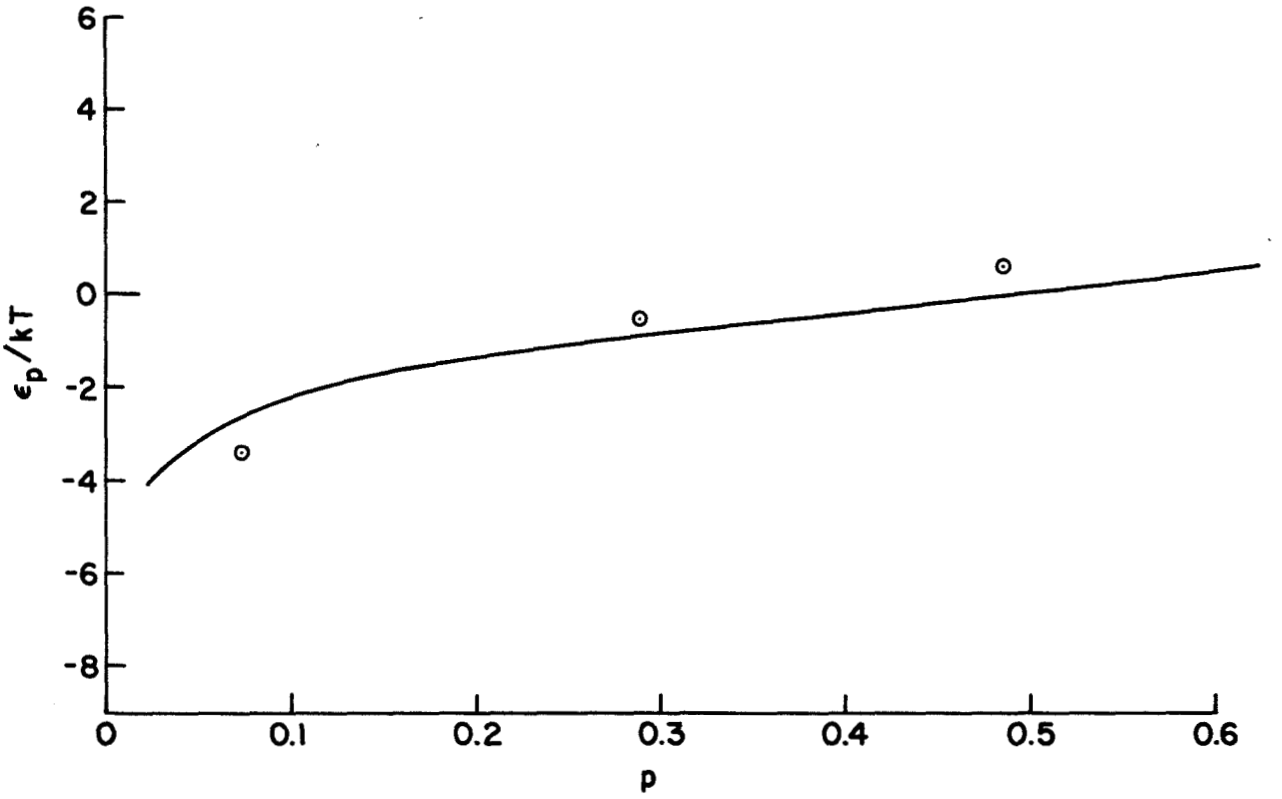

Figure 12. Data points show the variation of the position of the energy distribution peak h on the energy axis ϵ_p with p for the ⟨100⟩ direction of a zirconium-oxygen coated tungsten emitter, where d = 0.091 eV. Solid line is the theoretical curve based on a free-electron model.

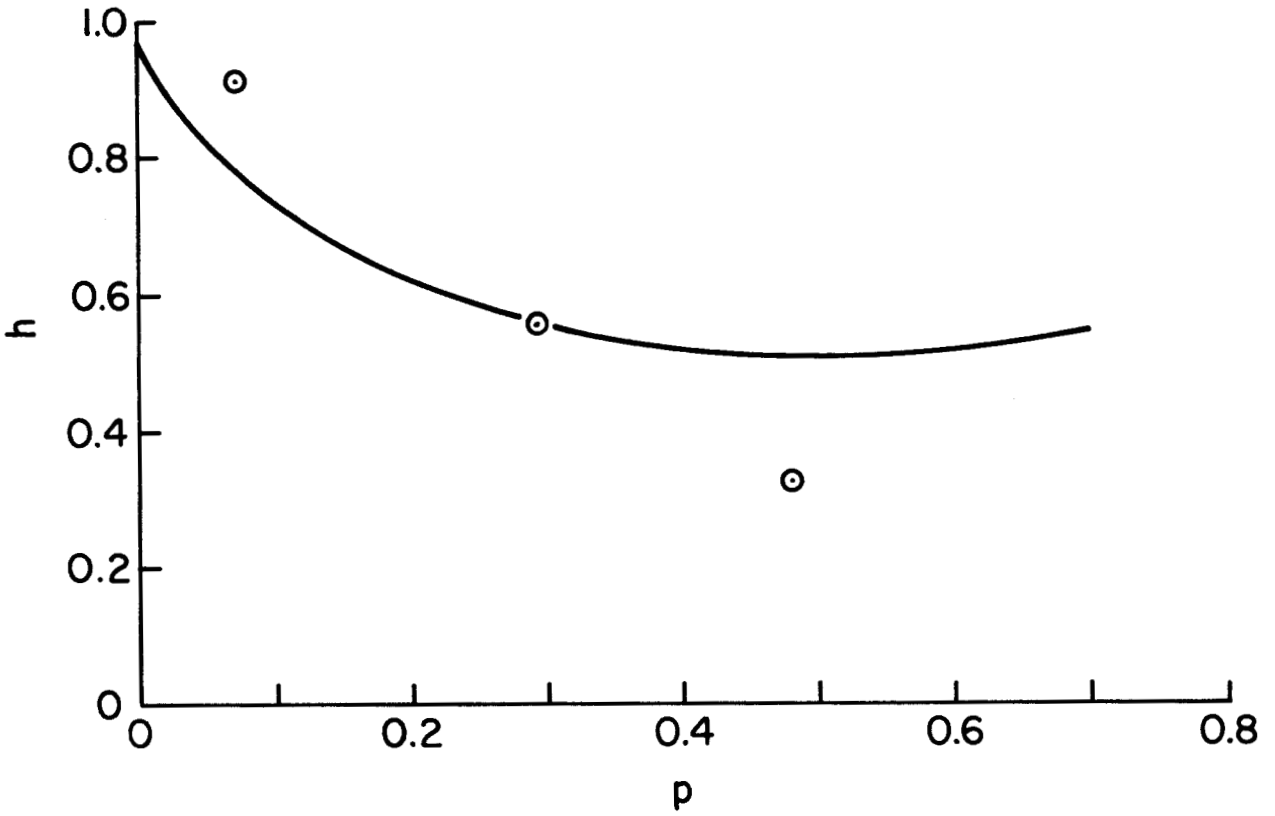

Figure 13. Data points show the variation of the total energy distribution peak height h with p for the ⟨100⟩ direction of a zirconium-oxygen coated tungsten emitter, where d = 091 eV. Solid line is the theoretical curve based on a free-electron model.

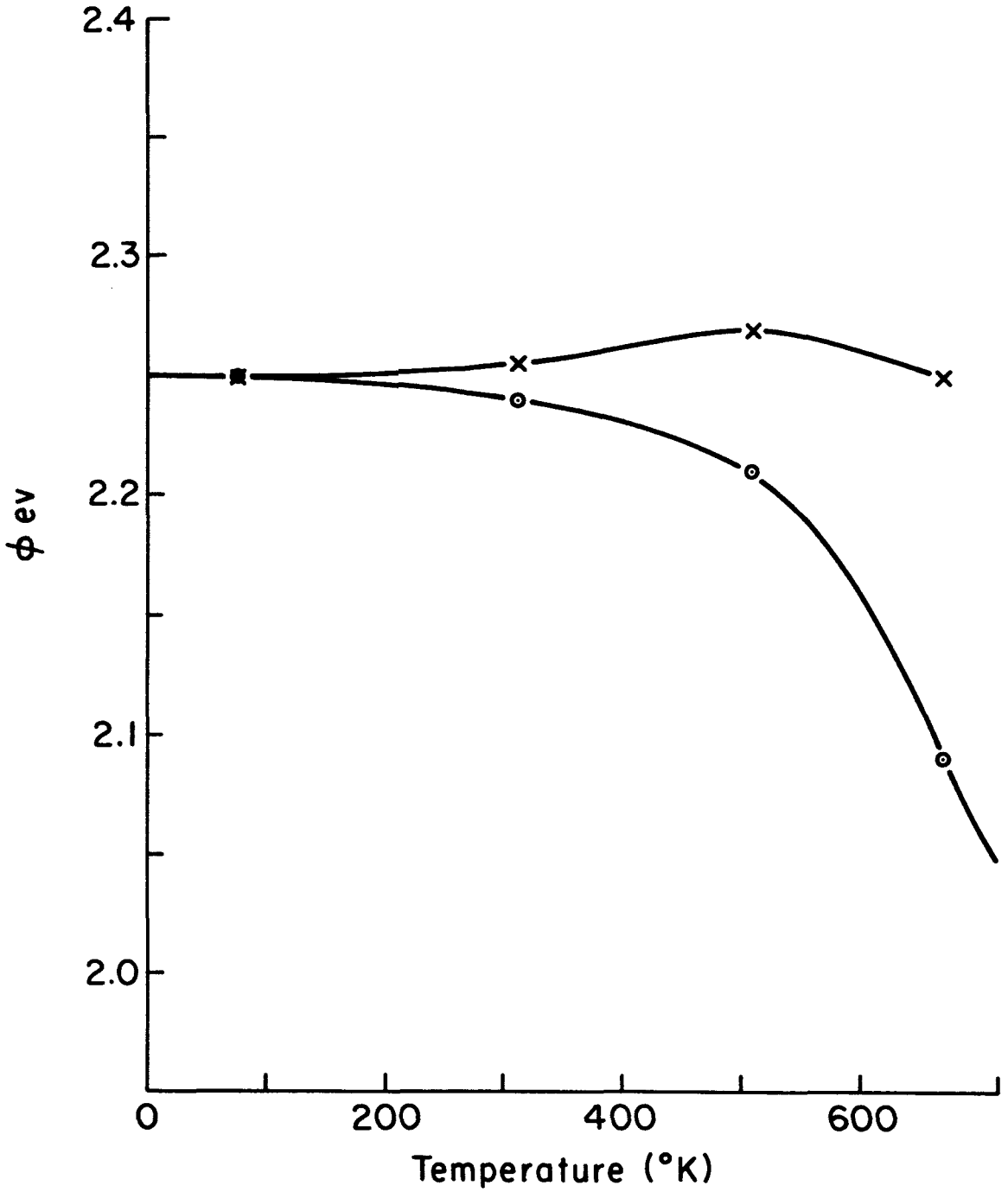

Figure 14. Curve (a) is the variation of the apparent work function of the (100) plane of a zirconium-oxygen coated tungsten emitter as determined by the Fowler-Nordheim slopes. Curve (b) gives the curve (a) results corrected for the T-F contribution to the field emission current.

In addition, work functions calculated from the energy distribution results are considerably lower than those calculated from the Fowler-Nordheim theory assuming a uniform field factor over the emitter. It was also found that the work function of the <100> plane of a zirconium-oxygen coated tungsten emitter was independent of temperature over the range of 77 to 675 $^{\circ}$K.

REFERENCES

1. Annual Report for Contract NASw-458 (Field Emission Corporation, April, 1963).

2. I. Langmuir & K. H. Kingdon, Physical Review, Vol. 34, 129 (1929).

3. Preprint, E. D. Wolf (North American Aviation Science Center, Thousand Oaks, California).

4. Annual Report for NAS3-2596 (Field Emission Corporation, June, 1964).

5. Quarterly Report No. 4 for Contract NASw-1082 (Field Emission Corporation, December, 1965).

6. R. Good and E. Müller, Handbuch der Physik 21, 176 (1956).

7. E. Müller, J. Appl. Phys., 26, 732 (1955).

8. L. Swanson and L. Crouser, Phys. Rev. Letters, 16, 389 (1966).

9. Quarterly Report No. 3 for Contract NASw-1082 (Field Emission Corporation, August, 1965).

10. Final Report for Contract DA36-039 SC90829 (Field Emission Corporation, June, 1964).